2023

Advanced Thermoluminescence Spectroscopy as a Research Tool for Semiconductor and Photonic Materials: A Review and Perspective

Farida Selim
Bowling Green State University, faselim@bgsu.edu

Repository Citation

Selim, Farida, "Advanced Thermoluminescence Spectroscopy as a Research Tool for Semiconductor and Photonic Materials: A Review and Perspective" (2023). *Physics and Astronomy Faculty Publications*. 19.
https://scholarworks.bgsu.edu/physics_astronomy_pub/19

physica status solidi a
www.pss-a.com

Advanced Thermoluminescence Spectroscopy as a Research Tool for Semiconductor and Photonic Materials: A Review and Perspective

Farida A Selim

Thermoluminescence (TL) or thermally stimulated luminescence (TSL) spectroscopy is based on liberating charge carriers from traps in the bandgap by providing enough thermal energy to overcome the potential barrier of the traps. It provides a powerful tool to measure the positions of the localized states/traps in the bandgap. Despite that, its applications in semiconductors are very limited. Herein, the basics of TL spectroscopy and the recent advances in the technique with focus on cryogenic thermally stimulated photoemission spectroscopy (C-TSPS) which extends TL measurements to cryogenic regime and allows the detection of very low concentrations of shallow and deep localized states is discussed. One goal herein is to introduce the reader to the use of TL and C-TSPS in the characterization of semiconductors, explaining how it can be applied and demonstrating its advantages as a powerful tool for measuring shallow donor/acceptor ionization energies in semiconductors and as a method for characterizing compensating defects. The article also discusses interesting potential applications of C-TSPS in new research areas such as corrosion and formation of oxide layers on metal surfaces.

1. Introduction

Point defects, impurities, and dopants often form localized states in the bandgap of electronic and photonic materials. The position of these localized states depends on many factors such as the charge state, size, and chemistry of these point defects[1] and it can be modified by external stimuli.[2] The positions or energy levels of these states in the bandgap dictate the electronic, optical, and electrical properties of bandgap materials[3,4] and it is vital to measure their energy levels/depths to understand and control the material properties. However, the available techniques for energy-level measurements are limited and often not suitable for many material systems.

It is useful to first distinguish between deep levels and shallow levels in terms of their impact and methods of detection. Point defects and impurities that occupy states close to the conduction and valence bands act as shallow donors and shallow acceptors, respectively, providing electron or hole conduction.[5–8] They also impact light emission and the optical properties of materials as they often act as trapping/detrapping points for charge carriers, greatly affecting exciton dynamics and light emission and luminescence from materials.[9,10] When point defects and dopants occupy states with deeper energies, little bit further from the conduction/valence band or midgap states, they act as deep donors/acceptors,[11,12] capturing and holding charge carriers at room temperature which may decrease or completely suppress both conductivity and light emission.[10,13] It is clear from the discussion that developing new sensitive techniques and advancing current techniques for detection of these localized states is crucial for characterizing and improving the properties of photonic and electronic materials and advancing their applications in many fields.

Only a handful of techniques are suitable for measuring shallow donor and acceptor ionization energies that occupy states close to the conduction or valence bands. Temperature-dependent (TD) Hall effect measurements from around 10 K to room temperature is the most common method for their measurements in semiconductors.[14–16] However, it is complex and fitting of the TD curve of the charge carrier density can be very challenging by the presence of multiple donor and acceptor species. Additionally, it is limited by geometry constraints and the need of making four contacts on the surface and cannot be used for resistive samples. Thus, powder, nonuniform shape, insulating, and resistive samples cannot be characterized by this technique. Electron paramagnetic resonance (EPR), photoluminescence (PL), and temperature dependent photoluminescence (TDPL) can be used to measure the donor/acceptor ionization energies.[17,18] However, their applications have been limited because of different factors such as the collapse of exciton and broadening of the PL peaks.[16] Deep-level transient spectroscopy

---

F. A. Selim
Department of Physics and Astronomy
Bowling Green State University
Bowling Green, OH 43403, USA
E-mail: faselim@bgsu.edu

F. A. Selim
Center for Photochemical Sciences
Bowling Green State University
Bowling Green, OH 43403, USA

The ORCID identification number(s) for the author(s) of this article can be found under https://doi.org/10.1002/pssa.202200712.

DOI: 10.1002/pssa.202200712

is the most common method for measuring deep trap levels in semiconductors.[19] However it can only measure trap levels with energy level more than 1 eV and it requires the fabrication of p–n junction or Schottky barrier as it works by applying forward/backward bias to inject majority or minority carriers into the depletion layer and measuring the capacitance.[20,21] Deep-level optical spectroscopy is another method for measuring deep traps, but also limited for traps with energy more than 1 eV.[22] Other methods for accessing the electronic signature of defects include positron annihilation spectroscopy (PAS)[23] and cathodoluminescence (CL).[24] PAS mainly reveals the nature, size, and charge state of defects.[25–27] However, temperature-dependent PAS can be effectively used to measure their activation energy.[28] CL is essentially useful to provide information on the distribution of traps as a function of depth and map quantum defects.[29] It is worth noting the difference between TL and CL. While TL gives the position of the localized states in the bandgap without information on their depth distribution, CL is a unique technique to probe the spatial distribution of defects in the samples.[30]

Thermoluminescence (TL) is a perfect tool for dosimetry and dating applications (e.g.,[31,32]); it is also a great tool for the detection of traps and measuring their energy levels.[33,34] Other methods based on thermally stimulated processes such as thermally stimulated conductivity (TSC) and thermally stimulated polarization and depolarization current can be also used to measure the trap levels.[35,36] TL or TSL has been widely applied for measuring deep and relatively shallow traps in optical and photonic materials[37,38] and has been quite useful for optical studies of single crystals, films, phosphors, and transparent ceramics for lasers, scintillators, and solid-state lighting applications and more.[9,39–53] However, its applications in semiconductors has not been realized until recently[5,8,54] and are still very limited. The goal of this article is to explain the basics of TL, inform the reader about its capability as a great tool for measuring the energy levels of donors and acceptors in semiconductors, and bring the attention to the development of cryogenic thermally stimulated photoemission spectroscopy (C-TSPS)[55] which extends TL or thermally stimulated emission measurements to cover the entire range of shallow and deep levels in bandgap materials. Examples on successful applications of TL for the characterization of deep and shallow donors and acceptors in semiconductors[56–60] are discussed in detail revealing how this technique can be a powerful tool in the study of the electrical transport properties of semiconductors. Finally, the potential applications of C-TSPS in new research areas such as corrosion, radiation damage, ion implantation, and defects in oxides and other bandgap materials are discussed.

2. Basics of TL and C-TSPS and Measurement Techniques

Theory of TL and long-period phosphorescence were introduced by Randall et al.[61] very early in 1945 and methods for finding the depths of electron traps in phosphors were developed. **Figure 1** explains the basics of TL mechanism in detail illustrating the different processes that take place and lead to emission. Four main processes take place: electron pumping to the conduction band leaving holes behind, electron and hole trapping at localized states, detrapping of electrons and holes by thermal stimulation, electron–hole recombination and photoemission. In many cases, after detrapping, electrons may be retrapped again; this will be discussed in detail below. TL mechanisms take place in bandgap materials if radiative recombination centers or activators centers are present. In standard TL, charge carriers are generated, and electrons are pumped to the conduction band at room temperature. Thus, electrons and holes are mostly trapped at deep states, which hinders the capability of the technique in detecting shallow levels.

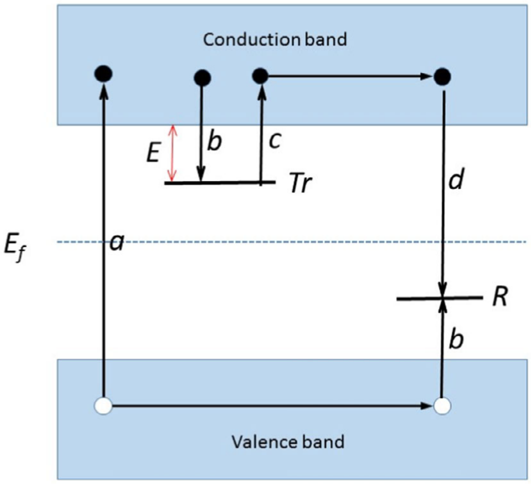

Figure 1. Schematic showing the simplified model of the mechanism of TL: a) electrons are pumped to the conduction band, b) electrons and holes are captured by trapping centers (Tr) and recombination centers (R), c) release of electrons from traps by thermal stimulation where they move through the conduction band, d) electrons and holes recombine through recombination centers. E_f: Fermi energy, E: trap depth. Reproduced under the terms of the CC-BY open access license.[34] Copyright 2017, The Authors, published by MDPI.

The basic idea of C-TSPS is to generate charge carriers at cryogenic temperature less than 10 K using a relevant photoexcitation source. The name of C-TSPS is more relevant than TL when photoemission may extend beyond visible light-to-ultraviolet and near-infrared regions. Two modes of excitations can be used; the first is photoexcitation source with energy above the bandgap energy to pump electrons from the valence to the conduction band. This can be xenon lamp, deuterium lamp, or X-ray source. Using high-energy photons is necessary for ultrawide-bandgap materials. The other mode is the use of photoexcitation energy within the bandgap to pump electrons from defect levels in the bandgap to the conduction band. Laser diodes or intense light-emitting diodes (LEDs) are good options for that. The selection of one of the two excitation modes is determined by the goal of the measurements. Since the excitation is carried out at 10 K, the electrons are captured by trapping centers, both in shallow and in deep states. Long photoexcitation time is necessary to fill up all available states. Releasing the charge carriers and emptying the traps is done by thermal sweep. As electrons and holes are released, they can lead to photoemission through several possible routes: their recombination (electron & hole), transferring their energy to luminescence centers, or capturing them by their original atoms. Collecting emission and measuring it as a function of temperature from 10 K up to room or higher temperature allow one to obtain the temperature-dependent emission known as glow curve.[62] Information on wavelength emission is useful in characterizing the emission or luminescence centers.

Photoemission can be collected in different ways. If all emitted photons regardless of their wavelength are collected simultaneously as a function of temperature, this method does not provide information about luminescence centers. To obtain spectral information, diffraction grating with a charge-coupled device (CCD)[63]may be used to record the spectrum at each temperature in a specific wavelength range (e.g., from UV to NIR) controlled by the diffraction grating setup. This may not be efficient for weak light emission and cannot detect the low-density traps in the material. In the recently developed C-TSPS,[55] a sensitive photomultiplier tube (PMT) connected to single-photon counter is used to capture any photoemission and achieve high-sensitivity trap detection. If spectral information is desirable with this setup, a monochromator is added before the PMT and accustomed to certain wavelengths. The measurements can be repeated at different wavelengths to explore the spectral range of the emission.

Analysis of the temperature-dependent emission or glow curve[35,64] in TL or C-TSPS can provide useful information, the energy levels (activation energies) of traps/defects, their density, capture cross section, and the degree of kinetics which is dependent on the trapping/detrapping processes. In first-order kinetics, the charge carriers give emission directly after their release from traps. This can be easily recognized from the asymmetric shape of the glow curve as shown in **Figure 2**. If the charge carriers are being retrapped, detrapped before giving emission, this represents second- or higher-order kinetics (Figure 2). If retrapping is slow, the kinetics is considered first order and the asymmetric shape of the glow curve is maintained. Many factors determine the degree of kinetics such as the proximity between the traps and emission centers in the system, the density of traps, the density of emission centers, and their spatial distributions in the material, and the mobility of charge carriers. In most situations, the glow curve forms of several overlapped peaks because of the presence of several traps with different transition levels. Deconvolution of the glow curve demands a rigorous analysis to resolve into its individual peaks and calculate the parameters of traps/localized states and several codes and algorithms have been developed to fit the glow curve and extract the parameters of the localized states.[65–70] Since the focus of this article is to review TL applications in semiconductors, demonstrate its advantages in this area, and guide the reader on data interpretation and their physical meaning, the mathematical description of TL and the different methods for trap parameter calculations will not be discussed here. For that, we refer the reader to Ref. [55] where the fitting and calculation procedures are explained in detail, showing all parameters that can be extracted from the glow curves. Further information on TL theory, analysis of complex glow curves, and the mathematical models of first-order, second-order, and higher-order kinetics can be found in Refs. [61,71–76]. The two common methods used to calculate the activation energy (depth) of traps, initial rise method, and variable heating rate method are well explained in the literature, see, e.g.,[35,37,64].

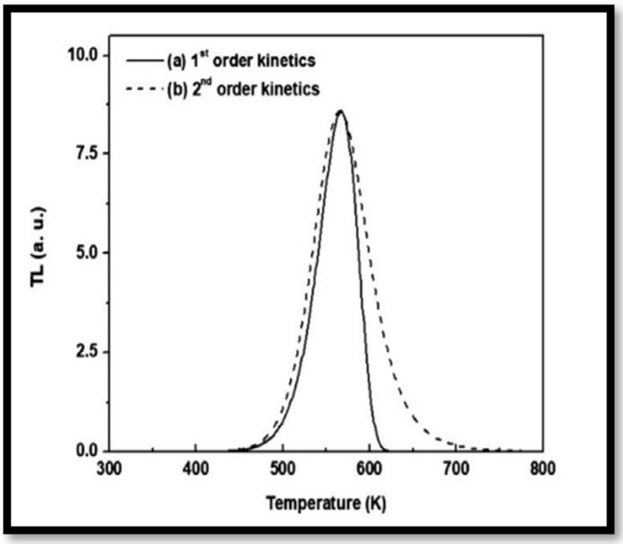

Figure 2. Graphic of TL glow curves illustrating first-order and second-order kinetics.

Before describing TL and C-TSPS applications in semiconductors, limitations of TL methods and possible challenges in glow curve analysis should be briefly discussed. In some materials, nonradiative recombination between electrons and holes can interfere with the radiative recombination process suppressing or decreasing the TL or photoemission. This represents the biggest drawback of the technique as it may hinder TL spectroscopy and prevent its applications in some materials.[77] Thermal quenching with increasing temperature may occur in some thermoluminescent materials, leading to a decrease in the TL intensity, and it may disturb the shape of the glow peaks. The simulation of its effects on the TL signal, shape of glow curve, and calculations of trap parameters is described in detail in Ref. [78].

3. Applications of TL and C-TSPS in Semiconductors

3.1. Measurements of Donor and Acceptor Ionization Energies in Semiconductors

Figure 3 shows schematics illustrating the measurements of donor and acceptor ionization energies by TSPS process. The existence of radiative emission centers in the material is a must for TL or C-TSPS. In oxide semiconductors, oxygen vacancies are often present and most likely lead to emission in the visible region. Other native defects and impurities in semiconductors may also act as photoemission centers. In n-type semiconductors, the conductivity is driven by electron conduction and shallow donors are dominant, occupying states close to the conduction band, as shown in Figure 3a. In C-TSPS when electrons are pumped from the valence to the conduction band at 10 K, they move through the conduction band until they are captured by the shallow donors, as shown in the figure. By providing energy through thermal sweep, the electron can escape the shallow donor to the conduction band and then recombine with holes at radiative recombination centers emitting photons. From the dependence of the emission on temperature, the ionization energy of the shallow donors can be calculated. In p-type semiconductor, the conductivity is driven by hole conduction and the

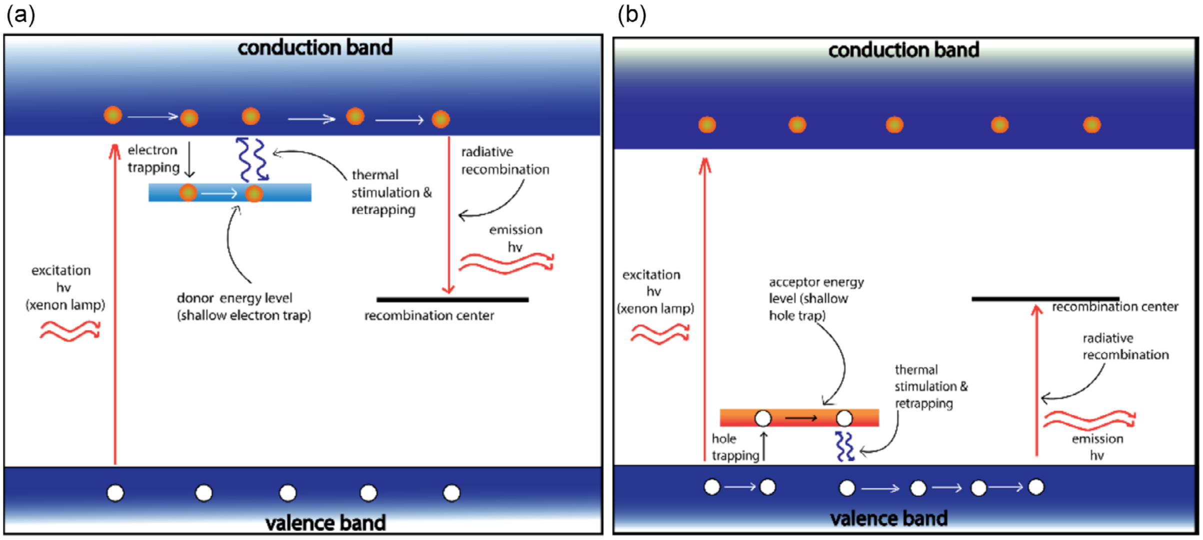

Figure 3. Schematics showing the detection mechanism for a) shallow donors and b) shallow acceptors in semiconductors by TSPS. Reproduced under the terms of the CC-BY open access license.[5] Copyright 2020, The Authors, published by Springer Nature.

shallow acceptors are positioned close to the valence band. After photoexcitation at 10 K, created holes may be trapped at these acceptor states, as shown in Figure 3b. By thermal stimuli, holes recombine with electrons in radiative centers, leading to photoemission at specific temperature. The ionization energy of the acceptor levels can be calculated as explained in the case of donors. From the temperature dependence of the emission, other important parameters such as the density of donors/acceptors and their capture cross sections can be calculated. One of the advantages of this method is its ability to detect many donor and acceptor species at the same time including both majority and minority carriers. Their relative densities in the material can be obvious from the difference in the intensities of the peaks. A limitation of this technique is its inability to distinguish between donors and acceptors. However, combining other measurements with TL allows us to easily identify the shallow traps as donors or acceptors.

The first application of TL in characterizing donors in semiconductors was carried on ZnO single crystals[8]where TL measurements from 77 K to room temperature revealed the ionization energies of three different hydrogen species in ZnO and solved a long-time controversial issue on the nature of H donors in ZnO. In that work, three hydrogen donor species were detected, and their ionization energies were obtained from their glow curves and found to be 36, 47, and 55 meV, which are consistent with the previously reported donor ionization energies in ZnO.[79–81] This work demonstrated the great capability of TL in the study of donors in semiconductors as it enabled identifying the three H donor species and measuring their ionization energies in a single experiment while each ionization energy was identified before using the different techniques which led to the controversy on the nature and ionization energy of H donors in ZnO. The 51 meV ionization energy was measured by TD Hall effect,[82] 35 meV by EPR,[18] and 47 meV by PL.[17] TL enabled the measurements of the three ionization energies and associated them with three different species of hydrogen[8] and the study further showed how to switch from one hydrogen specie to another.

Very recently TL was applied to measure both donor and acceptor ionization energies in the important emerging semiconductor Ga_2O_3[5] and further correlate their measurements with the electrical transport properties of Ga_2O_3 (**Figure** 4). These TSL measurements revealed the ionization energies of a novel acceptor forming Ga vacancy with 2H and novel donor forming Ga vacancy with 4H, associated with remarkable hole and electron conduction in Ga_2O_3. The nature and structure of the donors and acceptors were measured by PAS and their formation was verified by density function theory calculations.

3.2. Measurements of Density and Energy Level of Compensating Acceptors in Semiconductors

The electrical transport properties of semiconductors are often characterized by the resistivity, carrier density, and mobility. The carrier density "electron or hole concentration" should be equal to the dopant (donor or acceptor) concentrations. However, in many situations the electron density can be reduced or diminished by the presence of deep traps capturing electrons and acting as compensating acceptors. As mentioned in the Introduction, these deep traps can be measured by DLTS if p–n junction is made on the surface. Recently, TL has been applied to detect compensating acceptors in n-type Ga_2O_3 films grown by metal–organic chemical vapor deposition (MOCVD) and measure their density and depth in the bandgap.[56] The films were homoepitaxially grown on semi-insulating Fe-doped Ga_2O_3 single crystals and doped with Si to achieve n-type conductivity. Details on the film growth, structural characterization, and impurity measurements can be found in Ref. [57]. TL measurements were successful in the detection of deep traps in the film and calculating their density and energy level.[56] **Figure 5** shows an interesting correlation between these traps and film resistivity. The increase of their TL peak intensity with the increase in film resistivity clearly indicates their role as compensating acceptors. Their concentration per centimeter square was labeled as sheet trap number

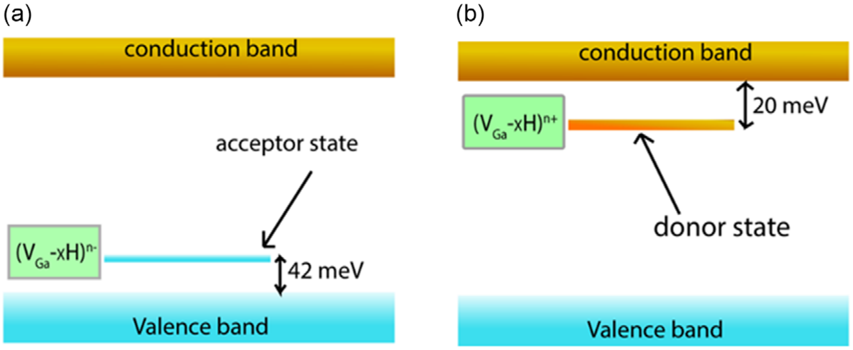

Figure 4. Ionization energies of hydrogen-related a) acceptors and b) donors in Ga_2O3 measured by TL Reproduced under the terms of the CC-BY open access license.[5] Copyright 2020, The Authors, published by Springer Nature.

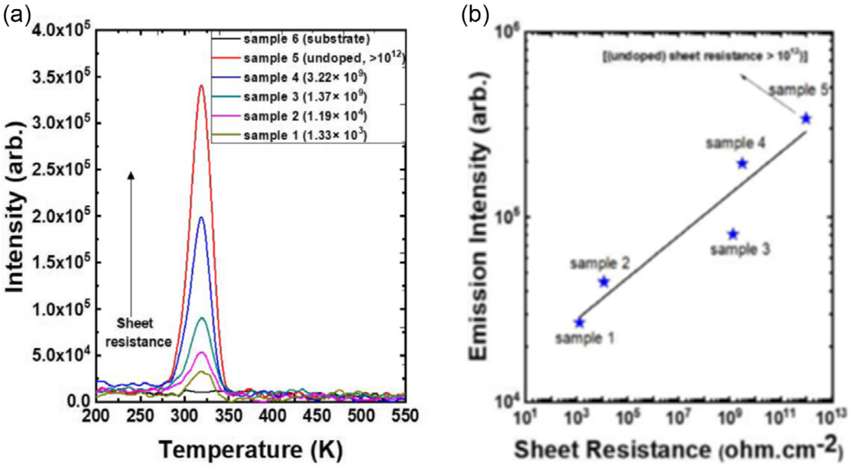

Figure 5. Detection of compensating acceptors in Ga_2O_3 films by TL. a) The TL glow curve shows the strong rise in emission with the increase in sheet resistance. The sheet resistance is given next to the sample label. b) TL peak intensity as a function of sheet resistance. Reproduced with permission.[56] Copyright 2020, The Authors, published by AIP Publisher.

adding a new parameter to the common electrical transport parameters, sheet carrier number (carrier concentration per cm^2), sheet resistance, and carrier mobility.

Spectral investigation of the TL emission from the resistive Si-doped Ga_2O_3 films revealed the interaction between the compensating acceptors and the radiative emission centers (**Figure 6**). The 3D TL emission as a function of temperature and wavelength in Figure 6 displays an emission peak around 700 nm. Previous studies[83,84] suggested that the 700 nm emission is common in oxides and associated with low level of Fe impurities. Fe impurities most likely diffused from the substrate into Ga_2O_3 film and acted as radiative recombination centers. The contour plot in Figure 6 shows a peak at 700 nm spreading over 100 nm, suggesting broad emission associated with more than one impurity or defect center.

3.3. Measurements of Defects and Impurities in Semiconductors

While the two applications described above are still in infancy and not well known, applications of TL in the detection of native and extrinsic defects associated with impurities have been relatively known with several TL measurements reported on important semiconductors such as ZnO and recently Ga_2O_3.[59,60] Most of these studies have identified deep traps but did not correlate them with the semiconducting properties; however, they demonstrate the effectiveness and relevance of TL in the study of defects in bulk crystal, film, powder, and nanoparticle semiconductors. TL has been applied very early to study ZnO before recognizing ZnO as a potential semiconductor for devices because of its strong emission and potential applications as phosphors, scintillators, and light emitters. Earlier studies identified the point defects and impurities that act as deep traps in ZnO powders and polycrystals.[85–89] Several studies also used TL and studied extrinsic defects induced by irradiation.[90–92] Recently with the increase interest in Ga_2O_3, TL was applied to characterize point defects in Ga_2O_3 and revealed the energy levels of several point defects and impurities often formed in Ga_2O_3 lattice.[59,60,93] An important finding from TL studies is that doping the crystals for instance by Fe or Mg significantly modified the levels of the original native traps in Ga_2O_3 probably due to the formation of complex defects. The measurements in Ref. [93] reveal the direct connection between the increase of trap density and the semi-insulating properties of the crystals. Other

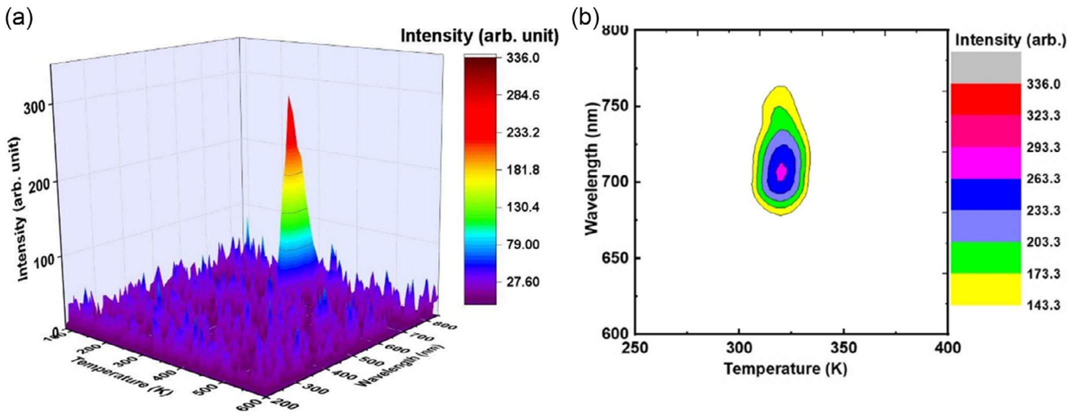

Figure 6. a): 3D TL emission as function of temperature and wavelength associated with the compensating acceptors and emission centers in n-type Ga_2O_3 films. b) Projection of the 3D graph on *x–y* plane showing the contour plot. Reproduced under the terms of the CC-BY open access license.[57] Copyright 2021, The Authors, published by Elsevier.

studies showed that a Cr^{3+} impurity provides a trap with energy of 0.55 eV below the conduction band, O-vacancy is associated with a trap with 0.94 eV, while O-vacancy with Cr^{3+} or Fe^{3+} defect complexes result in trap levels around 0.7 eV[59] and Fe^{2+}/Fe^{3+} was found to form a trap level at 0.84 eV.[60] The TL study in Ref. [59] further showed that the transition levels of Cr and associated defects in Ga_2O_3 strongly depend on the level of Cr doping (**Figure 7**). The trap structures in Cr doped Ga_2O_3 nanowires were also investigated by TL measurements.[94] With respect to other semiconductors such as Si and GaN, only few TL studies were reported Refs. [95,96]. In hydrogenated amorphous silicon (a-Si:H),[95]TL was applied in one study to investigate the nature of defects introduced by light soaking, γ-irradiation, hydrogen removal, and rehydrogenation and indeed revealed important information about them and showed that defects induced in all cases share similar character and nature.

4. New Potential Applications of TL and C-TSPS

Enhancing the capability of measuring very-low-density traps and extending the detection limit to ultrashallow traps through the use of C-TSPS open up possibilities to apply TL and thermally stimulated photoemission in new avenues such as corrosion, radiation damage, and ion implantation. While the focus of this article is to introduce the reader to the use of TL in semiconductor characterization, it is still worth to discuss some new uses that are enabled by the development of C-TSPS. One interesting example is detection of corrosion-related defects which may have great impact on material strength and behavior in many applications. Corrosion leads to formation of oxide layers on the metal surface in oxidizing environments; such layers containing a variety of point and extended defects impacting the material strength and corrosion rate and resistance.[97,98] C-TSPS can be effective in detecting the defects induced during the formation of oxide layers. To test that, Fe foil was immersed in water at 70 °C for 24 h, which led to the formation of different phases of Fe oxides on the surface, as shown in the X-ray diffraction (XRD) pattern (**Figure 8**).

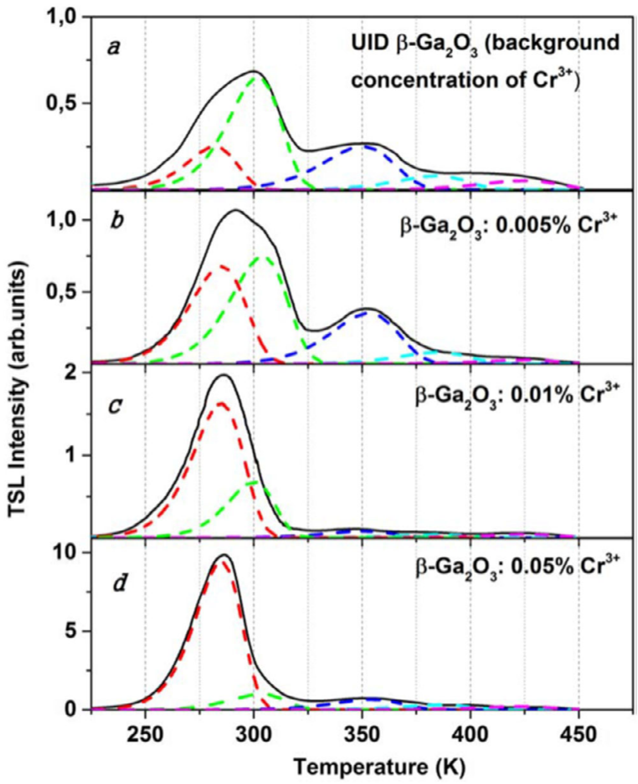

Figure 7. TL glow curves of β-Ga_2O_3 crystals doped with various concentrations of Cr. a) Background concentration of Cr^{3+}, b) 0.005% Cr^{3+}, c) 0.01% Cr^{3+}, and d) 0.05% Cr^{3+}. Reproduced under the terms of the CC-BY open access license.[59] Copyright 2020, The Authors, published by IOP Publishing.

C-TSPS measurements were used to examine the Fe foil after corrosion in water for 24 h. The foil was first photoexcited at 9 K using a deuterium lamp for 15 min. After that, the lamp was turned off and the light was collected using a monochromator setting at 450 nm during thermal sweep from 9 to 300 K. The glow curve in **Figure 9** reveals several overlapped peaks indicating the presence of different trap levels formed in the oxide

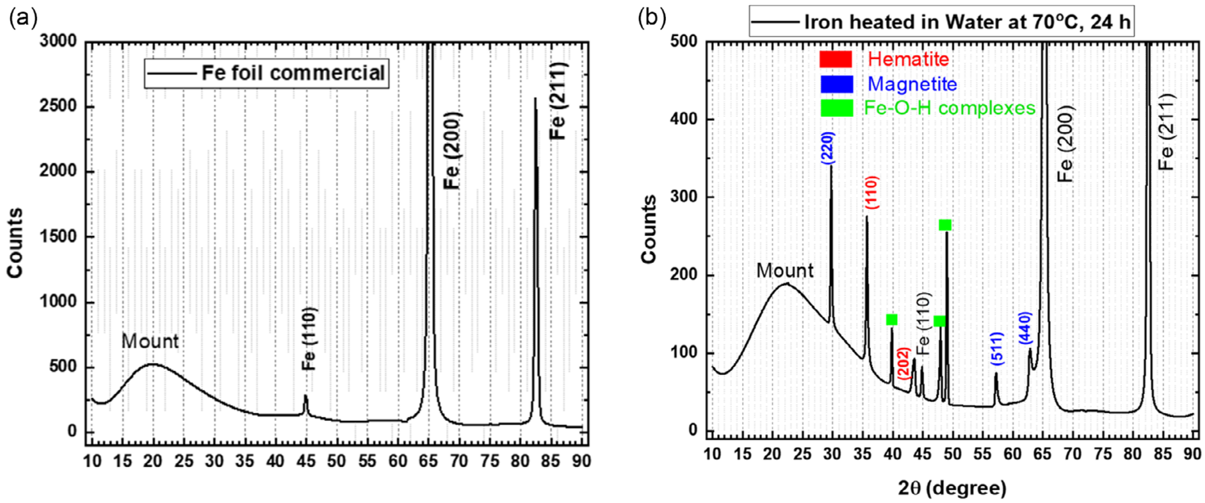

Figure 8. XRD pattern of Fe foil before a) and after b) heating in water at 70C for 24 h. Heating in water led to the formation of Fe oxide phases.

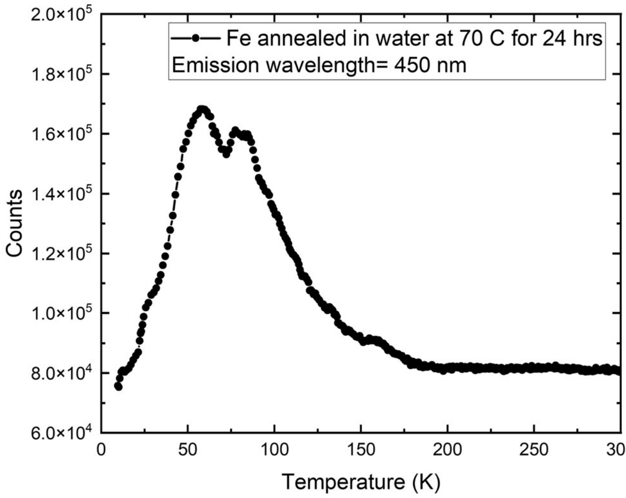

Figure 9. TSPS after heating Fe foil in water at 70 °C for 24 h. The emission monochromator was set at 450 nm. The glow curve shows the formation of several trap levels associated with corrosion-related defects in the oxide layers formed at the surface.

layers associated with corrosion-induced defects. These measurements illustrate the capability of C-TSPS of detecting formation of oxides and structural changes during corrosion. By monitoring the change of emission intensity after varied corrosion time, the measurements may be utilized to estimate corrosion rate. In addition, they can detect the defects formed in the oxide layers and then enable the investigation of their effects on corrosion resistance and species transport. C-TSPS can be also an effective method in characterizing point defects induced by irradiation and ion impanation.

5. Conclusion

The principles of TL in measuring localized states and the recent developments in C-TSPS are explained and various examples of its applications in characterizing semiconductors are discussed.

Extending TSPS to the cryogenic regime enables the detection of ultrashallow traps and the use of sensitive PMTs and single-photon counting allows one to efficiently measure the low-density traps in the bandgap. The few examples of applying TL on ZnO and Ga_2O_3 illustrate the capability of the technique and its potential as an important tool in the study of semiconductors and oxides in addition to its common applications in optical and photonic materials. Potential applications of C-TSPS in investigating corrosion-induced defects are demonstrated.

Acknowledgements

The author would like to thank Sahil Agarwal and Minhazul Islam for their help in preparing the schematic diagrams and graphs. The author acknowledges support from 1) Thermal Energy Transport under Irradiation (TETI), an Energy Frontier Research Center funded by the US Department of Energy (DOE), Office of Science, Office of Basic Energy Sciences; 2) Fundamental Understanding of Transport Under Reactor Extremes (FUTURE), an Energy Frontier Research Center funded by the DOE, Office of Science, Basic Energy Sciences; and 3) the National Science Foundation (NSF) under grant number DMR-2005064.

Conflict of Interest

The author declares no conflict of interest.

Keywords

corrosion, donors/acceptors, Ga_2O_3, ionization energies, point defects, trap levels, ZnO

Received: October 16, 2022
Revised: January 28, 2023
Published online: March 8, 2023

---

[1] P. Erhart, K. Albe, A. Klein, *Phys. Rev. B* **2006**, *73*, 205203.
[2] D. Rana, S. Agarwal, M. Islam, A. Banerjee, B. P. Uberuaga, P. Saadatkia, P. Dulal, N. Adhikari, M. Butterling, M. O. Liedke, A. Wagner, F. A. Selim, *Phys. Rev. B* **2021**, *104*, 245208.

[3] M. Fasoli, A. Vedda, M. Nikl, C. Jiang, B. P. Uberuaga, D. A. Andersson, K. J. McClellan, C. R. Stanek, *Phys. Rev. B* **2011**, *84*, 081102.
[4] D. Winarski, C. Persson, F. A. Selim, *Appl. Phys. Lett.* **2014**, *105*, 221110.
[5] M. M. Islam, M. O. Liedke, D. Winarski, M. Butterling, A. Wagner, P. Hosemann, Y. Wang, B. Uberuaga, F. A. Selim, *Sci. Rep.* **2020**, *10*, 6134.
[6] M. Yamaga, E. G. Víllora, K. Shimamura, N. Ichinose, M. Honda, *Phys. Rev. B* **2003**, *68*, 155207.
[7] Z. Galazka, R. Uecker, K. Irmscher, M. Albrecht, D. Klimm, M. Pietsch, M. Brützam, R. Bertram, S. Ganschow, R. Fornari, *Cryst. Res. Technol.* **2010**, *45*, 1229.
[8] J. Ji, L. A. Boatner, F. A. Selim, *Appl. Phys. Lett.* **2014**, *105*, 41102.
[9] D. T. Mackay, C. R. Varney, J. Buscher, F. A. Selim, *J. Appl. Phys.* **2012**, *112*, 023522.
[10] A. Vedda, D. Di Martino, M. Martini, J. Mares, E. Mihokova, M. Nikl, N. Solovieva, K. Blazek, K. Nejezchleb, *Radiat. Meas.* **2004**, *38*, 673.
[11] G. F. Neumark, K. Kosai, *Anonymous Semiconductors and Semimetals*, Elsevier, Amsterdam **1983**, pp. 1–74.
[12] S. D. Mahanti, K. Hoang, S. Ahmad, *Phys. B* **2007**, *401*, 291.
[13] D. J. Winarski, W. Anwand, A. Wagner, P. Saadatkia, F. A. Selim, M. Allen, B. Wenner, K. Leedy, J. Allen, S. Tetlak, D. C. Look, *AIP Adv.* **2016**, *6*, 095004.
[14] A. Schildknecht, R. Sauer, K. Thonke, *Phys. B* **2003**, *340–342*, 205.
[15] F. A. Selim, M. C. Tarun, D. E. Wall, L. A. Boatner, M. D. McCluskey, *Appl. Phys. Lett.* **2011**, *99*, 202109.
[16] D. C. Look, J. W. Hemsky, J. R. Sizelove, *Phys. Rev. Lett.* **1999**, *82*, 2552.
[17] E. V. Lavrov, F. Herklotz, J. Weber, *Phys. Rev. B* **2009**, *79*, 165210.
[18] D. M. Hofmann, A. Hofstaetter, F. Leiter, H. Zhou, F. Henecker, B. K. Meyer, S. B. Orlinskii, J. Schmidt, P. G. Baranov, *Phys. Rev. Lett.* **2002**, *88*, 045504.
[19] D. V. Lang, *J. Appl. Phys.* **1974**, *45*, 3023.
[20] A. R. Peaker, V. P. Markevich, J. Coutinho, *J. Appl. Phys.* **2018**, *123*, 161559.
[21] D. Wickramaratne, C. E. Dreyer, B. Monserrat, J. Shen, J. L. Lyons, A. Alkauskas, C. G. Van de Walle, *Appl. Phys. Lett.* **2018**, *113*, 192106.
[22] J. Chen, W. Huang, H. Qu, Y. Zhang, J. Zhou, B. Chen, X. Zou, *Appl. Phys. Lett.* **2022**, *120*, 212105.
[23] R. Krause-Rehberg, H. S. Leipner, *Positron Annihilation in Semiconductors: Defect Studies*, Springer Science & Business Media, Berlin **1999**.
[24] T. M. Børseth, B. G. Svensson, A. Y. Kuznetsov, P. Klason, Q. X. Zhao, M. Willander, *Appl. Phys. Lett.* **2006**, *89*, 262112.
[25] M. H. Weber, F. A. Selim, D. Solodovnikov, K. G. Lynn, *Appl. Surf. Sci.* **2008**, *255*, 68.
[26] F. A. Selim, D. Winarski, C. R. Varney, M. C. Tarun, J. Ji, M. D. McCluskey, *Results Phys.* **2015**, *5*, 28.
[27] F. A. Selim, C. R. Varney, M. C. Tarun, M. C. Rowe, G. S. Collins, M. D. McCluskey, *Phys. Rev. B: Condens. Matter Mater. Phys.* **2013**, *88*.
[28] K. E. Knutsen, A. Galeckas, A. Zubiaga, F. Tuomisto, G. C. Farlow, B. G. Svensson, A. Y. Kuznetsov, *Phys. Rev. B* **2012**, *86*, 121203.
[29] G. C. Vasquez, M. E. Bathen, A. Galeckas, C. Bazioti, K. M. Johansen, D. Maestre, A. Cremades, Ø. Prytz, A. M. Moe, A. Y. Kuznetsov, L. Vines, *Nano Lett.* **2020**, *20*, 8689.
[30] L. J. Brillson, H. L. Mosbacker, D. L. Doutt, Y. Dong, Z. Fang, D. C. Look, G. Cantwell, J. Zhang, J.J. Song, *Superlattices Microstruct.* **2009**, *45*, 206.
[31] A. Bos, *Nucl. Instrum. Methods Phys. Res. Sect. B* **2001**, *184*, 3.
[32] A. J. J. Bos, *Radiat. Meas.* **2006**, *41*, S45.
[33] P. Saadatkia, C. Varney, F. Selim, *Luminescence-An Outlook on the Phenomena and their Applications*, InTech, Croatia **2016**.
[34] A. J. Bos, *Materials* **2017**, *10*, 1357.
[35] R. Chen, S. W. McKeever, Theory of Thermoluminescence and Related Phenomena, World Scientific, Singapore **1997**.
[36] B. Wang, P. Saadatkia, F. A. Selim, D. Look, *J. Electron. Mater.* **2018**, *47*, 604.
[37] C. R. Varney, D. T. Mackay, A. Pratt, S. M. Reda, F. A. Selim, *J. Appl. Phys.* **2012**, *111*, 063505.
[38] W. L. Medlin, *J. Chem. Phys.* **1963**, *38*, 1132.
[39] S. Agarwal, M. S. Haseman, A. Khamehchi, P. Saadatkia, D. J. Winarski, F. A. Selim, *Opt. Mater. Express* **2017**, *7*, 1055.
[40] L. Zhang, J. Wu, P. Stepanov, M. Haseman, T. Zhou, D. Winarski, P. Saadatkia, S. Agarwal, F. A. Selim, H. Yang, Q. Zhang, Y. Wang, C. Wong, H. Chen, *Photonics Res.* **2019**, *7*, 549.
[41] F. A. Selim, A. Khamehchi, D. Winarski, S. Agarwal, *Opt. Mater. Express* **2016**, *6*, 3704.
[42] A. Kumar Choubey, N. Brahme, *Open Nanosci. J.* **2011**, *5*, 41.
[43] O. Hai, X. He, M. Pei, X. Wu, Q. Ren, Improving Afterglow Properties of Sral2o4: Eu2, Dy3 by Changing the Morphology of Silver Nanoparticles. Dy3 by Changing the Morphology of Silver Nanoparticles.
[44] Y. Murayama, S. Watanabe, M. Akase, K. Matsui, *J. Lumin.* **2022**, *251*, 119248.
[45] S. M. Reda, C. R. Varney, F. A. Selim, *Results Phys.* **2012**, *2*, 123.
[46] N. M. Trindade, E. P. Silva, M. Nunes, J. M. Munoz, J. Santos, E. M. Yoshimura, R.S. Silva, *Opt. Mater.* **2020**, *108*, 110181.
[47] E. A. Canaza-Mamani, N. F. Cano, J. Mosqueira-Yauri, T. G. Rao, S. C. Aynaya-Cahui, A. J. Gonsalez-Vasquez, M. B. Gomes, J. F.D. Chubaci, S. Watanabe, J. S. Ayala-Arenas, *J. Lumin.* **2022**, *245*, 118585.
[48] Q. Liu, Q. Yang, G. Zhao, S. Lu, *J. Alloys Compd.* **2014**, *582*, 754.
[49] M. S. Holston, I. P. Ferguson, N. C. Giles, J. W. McClory, D. J. Winarski, J. Ji, F.A. Selim, L.E. Halliburton, *J. Lumin.* **2016**, *170*, 17.
[50] T. Aitasalo, J. Hölsä, H. Jungner, M. Lastusaari, J. Niittykoski, *J. Phys. Chem. B* **2006**, *110*, 4589.
[51] Q. Liu, Q. H. Yang, G. G. Zhao, S. Z. Lu, H. J. Zhang, *J. Alloys Compd.* **2013**, *579*, 259.
[52] A. Vedda, D. Di Martino, M. Martini, V. V. Laguta, M. Nickl, E. Mihokova, J. Rosa, K. Nejezchleb, K. Blazek, *Phys. Status Solidi A* **2003**, *195*, R1.
[53] Y. Kitagawa, J. Ueda, S. Tanabe, *Phys. Status Solidi A* **2022**, *219*, 2100670.
[54] M. S. Haseman, P. Saadatkia, J. T. Warfield, J. Lawrence, A. Hernandez, G. E. Jellison, L. A. Boatner, F. A. Selim, *J. Electron. Mater.* **2018**, *47*, 1497.
[55] M. M. Islam, M. Bakr, J. N. Aboa, F. A. Selim, *J. Appl. Phys.* **2021**, *130*, 033104.
[56] M. M. Islam, N. Adhikari, A. Hernandez, A. Janover, S. Novak, S. Agarwal, C. L. Codding, M. Snure, M. Huang, F. A. Selim, *J. Appl. Phys.* **2020**, *127*, 145701.
[57] A. Hernandez, M. M. Islam, P. Saddatkia, C. Codding, P. Dulal, S. Agarwal, A. Janover, S. Novak, M. Huang, T. Dang, M. Snure, F.A. Selim, *Results Phys.* **2021**, *25*, 104167.
[58] P. Saadatkia, S. Agarwal, A. Hernandez, E. Reed, I. D. Brackenbury, C. L. Codding, M. O. Liedke, M. Butterling, A. Wagner, F. A. Selim, *Phys. Rev. Mater.* **2020**, *4*, 104602.
[59] A. Luchechko, V. Vasyltsiv, L. Kostyk, O. Tsvetkova, B. Pavlyk, *ECS J. Solid State Sci. Technol.* **2020**, *9*, 045008.
[60] C. A. Lenyk, T. D. Gustafson, L. E. Halliburton, N. C. Giles, *J. Appl. Phys.* **2019**, *126*, 245701.
[61] J. T. Randall, M. H. F. Wilkins, *Proc. R. Soc. London Ser. A* **1945**, *184*, 365.
[62] M. Puchalska, P. Bilski, *Radiat. Meas.* **2006**, *41*, 659.

[63] M. J. Howes, D. V. Morgan, *Charge-Coupled Devices and Systems*, Wiley, New York **1979**.
[64] S. W. McKeever, *Thermoluminescence of Solids*, Cambridge University Press, Cambridge **1988**.
[65] Y. S. Horowitz, L. Oster, G. Reshes, D. Nemirovsky, D. Ginzburg, S. Biderman, Y. Bokobza, M. Sterenberg, I. Eliyahu, *Radiat. Prot. Dosimet.* **2022**, *198*, 821.
[66] M. Wazir-ud-Din, M. M. Mahmood, K. Ahmad, S. Hayat, M. T. Siddique, M. B. Kakakhel, S. M. Mirza, *Appl. Radiat. Isot.* **2022**, *179*, 110014.
[67] J. F. Benavente, J. M. Gómez-Ros, A. M. Romero, *Appl. Radiat. Isot.* **2019**, *153*, 108843.
[68] G. Kitis, J. M. Gomez-Ros, *Nucl. Instrum. Methods Phys. Res. Sect. A* **2000**, *440*, 224.
[69] G. Kitis, J. M. Gomez-Ros, J. W. Tuyn, *J. Phys. D* **1998**, *31*, 2636.
[70] K. S. Chung, H. S. Choe, J. I. Lee, J. L. Kim, S. Y. Chang, *Radiat. Prot. Dosimet.* **2005**, *115*, 343.
[71] G. Garlick, A. F. Gibson, *Proc. Phys. Soc.* **1948**, *60*, 574.
[72] E. I. Adirovitch, *J. Phys. Radium* **1956**, *17*, 705.
[73] C. E. May, J. A. Partridge, *J. Chem. Phys.* **1964**, *40*, 1401.
[74] R. R. Haering, E. N. Adams, *Phys. Rev.* **1960**, *117*, 451.
[75] S. W. McKeever, *Phys. Status Solidi A* **1980**, *62*, 331.
[76] G. Kitis, R. Chen, V. Pagonis, *Phys. Status Solidi A* **2008**, *205*, 1181.
[77] U. Erdem, *Sigma J. Eng. Natl. Sci.* **2015**, *33*, 421.
[78] B. Subedi, G. Kitis, V. Pagonis, *Phys. Status Solidi A* **2010**, *207*, 1216.
[79] E. V. Lavrov, *Phys. B* **2009**, *404*, 5075.
[80] B. K. Meyer, J. Sann, D. M. Hofmann, C. Neumann, A. Zeuner, *Semicond. Sci. Technol.* **2005**, *20*, S62.
[81] D. C. Look, D. C. Reynolds, J. R. Sizelove, R. L. Jones, C. W. Litton, G. Cantwell, W.C. Harsch, *Solid State Commun* **1998**, *105*, 399.
[82] A. R. Hutson, *Phys. Rev.* **1957**, *108*, 222.
[83] C. R. Varney, M. A. Khamehchi, J. Ji, F. A. Selim, *Rev. Sci. Instrum.* **2012**, *83*, 103112.
[84] S. R. Rotman, C. Warde, H. L. Tuller, J. Haggerty, *J. Appl. Phys.* **1989**, *66*, 3207.
[85] M. A. Seitz, W. F. Pinter, W. M. Hirthe, *Mater. Res. Bull.* **1971**, *6*, 275.
[86] D. De Muer, W. Maenhout-Van der Vorst, *Physica* **1968**, *39*, 123.
[87] U. Pal, R. Melendrez, V. Chernov, M. Barboza-Flores, *Appl. Phys. Lett.* **2006**, *89*, 183118.
[88] H. A. Borbón-Nuñez, C. Cruz-Vázquez, R. Bernal, G. Kitis, C. Furetta, V. M. Castaño, *Opt. Mater.* **2014**, *37*, 398.
[89] D. Zwingel, *J. Lumin.* **1972**, *5*, 385.
[90] V. A. Nikitenko, K. E. Tarkpea, I. V. Pykanov, S. G. Stoyukhin, *J. Appl. Spectrosc.* **2001**, *68*, 502.
[91] S. Bhushan, D. Diwan, S. P. Kathuria, *Phys. Status Solidi A* **1984**, *83*, 605.
[92] D. Diwan, S. Bhushan, S. P. Kathuria, *Cryst. Res. Technol.* **1984**, *19*, 1265.
[93] M. M. Islam, D. Rana, A. Hernandez, M. Haseman, F. A. Selim, *J. Appl. Phys.* **2019**, *125*, 055701.
[94] Y. Lu, F. Liu, Z. Gu, Z. Pan, *J. Lumin.* **2011**, *131*, 2784.
[95] S. Nikum, M. Banerjee, P. B. Vidyasagar, S. V. Bhoraskar, S. Babras, *Solid State Commun.* **1991**, *80*, 563.
[96] X. Zhengye, C. Jinmin, L. Yongqiang, W. Wenhua, Thermoluminescence of GaN-Based Blue Light-Emitting Diode (LED) Chips. **2014**.
[97] H. Kim, M. R. Chancey, T. Chung, I. Brackenbury, M. O. Liedke, M. Butterling, E. Hirschmann, A. Wagner, J. K. Baldwin, B. K. Derby, N. Li, K. H. Yano, D. J. Edwards, Y. Wang, F. A. Selim, *J. Appl. Phys.* **2022**, *132*, 105901.
[98] L. Ma, F. Wiame, V. Maurice, P. Marcus, *Npj Mater. Degrad.* **2019**, *3*.

Farida A Selim is professor of Physics and a member of the Center for Photochemical Science at Bowling Green State University. She has a broad research program in the field of semiconductors and electronic and photonic materials and has been active in constructing beam lines and developing new instrumentation for material characterization. She published 135 peer-reviewed journal articles, two books, and seven patents. She serves on the advisory boards of six international scientific committees related to positron annihilation, oxide semiconductors, photonic materials, and radiation. She plays leading roles in national research projects including two energy frontier research centers (EFRCs) from Department of Energy.